TR F6174

Bestemmelse av frysepunkt til natrium-/magnesiumklorid løsninger

Håvard Rekstad, Vidar Hardarsson

www.energy.sintef.no

SINTEF Energiforskning AS

Juni 2005

SINTEF

SINTEF

SINTEF Energiforskning AS

Postadresse: 7465 Trondheim
Resepsjon: Sem Sælands vei 11
Telefon: 73 59 72 00
Telefaks: 73 59 72 50

www.energy.sintef.no

Foretaksregisteret:
NO 939 350 675 MVA

TEKNISK RAPPORT

SAK/OPPGAVE (tittel)

Bestemmelse av frysepunkt til natrium-/ magnesiumklorid løsninger.

SAKSBEARBEIDER(E)

Håvard Rekstad, Vidar Hardarson

OPPDRAGSGIVER(E)

Veg- og trafikkfaglig senter, Vegdirektoratet Trondheim
Faggruppe Drift og vedlikehold. Abelsgate 5, 7030 Trondheim

TR NR.	DATO	OPPDRAGSGIVER(E)S REF.	PROSJEKTNR.
F6174	2005-06-21	Kai Rune Lysbakken	16x549

ELEKTRONISK ARKIVKODE	PROSJEKTANSVARLIG (NAVN, SIGN.)	GRADERING
050621141159	Petter Nekså	Fortrolig

ISBN NR.	RAPPORTTYPE	FORSKNINGSSJEF (NAVN, SIGN.)	OPPLAG	SIDER
82-594-2884-9		Inge R. Gran	3	8 + vedlegg

AVDELING	BESØKSADRESSE	LOKAL TELEFAKS
Energiprosesser	Kolbjørn Hejes v. 1D	73593950

RESULTAT (sammendrag)

Statens vegvesen gjennomfører et prosjekt der blanding av natriumklorid (NaCl) og magnesiumklorid ($MgCl_2$) brukes i vinterdriften. Magnesiumklorid anvendes for å senke NaCl-H_20 blandingens frysepunkt.

Det var ønskelig å bestemme en fasekurve som viser ved hvilken temperatur utfrysningen av is starter for løsninger med forskjellig konsentrasjon og et fast vektforhold mellom NaCl og $MgCl_2$ på 70/6.

Oppgaven ble løst både teoretisk og eksperimentelt. Standardavvik for differanse mellom målt og beregnet var 0,13 °C. Største differanse var -0.2 °C.

STIKKORD

EGENVALGTE		
	Frysepunkt	$MgCl_2$
	NaCl	H_2O

INNHOLDSFORTEGNELSE

Side

1 BAKGRUNN

Statens vegvesen gjennomfører et prosjekt der blanding av natriumklorid (NaCl) og magnesiumklorid ($MgCl_2$) brukes i vinterdriften. Magnesiumklorid anvendes for å senke NaCl-H_20 blandingens frysepunkt. Fasekurver for enkeltsaltløsninger var tilgjengelig men ikke for løsninger med begge saltene. Det var ønskelig å bestemme en fasekurve som viser ved hvilken temperatur utfrysningen av is starter for løsninger med forskjellig konsentrasjon og et fast vektforhold mellom NaCl og $MgCl_2$ på 70/6.

2 AKTIVITETER

Prosjektet var todelt og besto av å:

- Vurdere en teoretisk løsning av oppgaven.
- Finne aktuell del av fasekurven eksperimentelt.

3 LITTERATURDATA

Et litteratursøk ble gjort i fagdatabasen Compendex. En relevant artikkel ble funnet, Dubois (1997) vedlegg 2, hvor en beregningsmåte for startfrysetemperatur for løsning av NaCl og $MgCl_2$ i vann var gitt.

Ligningen, $T_{fi} = \sum_{i=0}^{2}\sum_{j=0}^{2} a_{ij} m_{NaCl}^{i} m_{MgCl_2}^{j}$, var basert på 2. grads polynom tilpasning til måleverdier

hvor a_{ij} er tilpasningskoeffisienter og m_{NaCl} og m_{MgCl2} molaliteten (mol salt /kg løsningsmiddel) for saltene. En mer detaljert beskrivelse er gitt i vedlegg 2.

Gyldighetsområde for ligningen er begrenset til konsentrasjon fra 0 opp til konsentrasjon tilsvarende hvert salts, eller blandingens, eutektiske blandingsforhold. Ligningens nøyaktighet i forhold til gitte eksperimentelle verdier oppgis til ± 0,5 °C for $MgCl_2$-H_2O og ± 0,2 °C for NaCl-H_20. En verifikasjon mot Melinder (1997) ble foretatt hvor oppgitt nøyaktighet ble bekreftet.

Det ble også funnet en artikkel Spencer (1990) hvor det syntes som om alle fasegrensene kunne beregnes. Men siden Dubois (1997) dekket problemstillingen aktuell i dette prosjektet ble den ikke benyttet.

4 MATERIALER OG METODE

Målingene ble utført iht. standard ASTM D 1177-94, ”Standard Test Method for Freezing Point of Aqueous Engine Coolants”, vedlegg 3. Eneste unntak fra standarden var at den spesifiserte tørris (CO_2) som kjølemiddel, mens det i forsøkene ble benyttet en spritkjøler som holdt temperaturen konstant på – 40 °C.

Saltene benyttet i forsøkene ble levert av oppdragsgiver mens tappevann i vårt laboratorium ble brukt som løsningsmiddel. NaCl var av type havsalt fra G.C.Rieber Salt AS mens $MgCl_2$ var løst i $MgCl_2$-6H20 (krystallvann) fra AKZO NOBEL. Det ble opplyst av oppdragsgiver at det skulle være 45 % $MgCl_2$ innhold i $MgCl_2$-$6H_20$. Usikkerhet om saltenes sammensetning kan gi en usikkerhet mht. sammenligning mellom målinger og beregninger. Saltenes fuktinnhold kan også påvirke resultatet. Fuktinnhold i NaCl ble målt og 2 tester viste henholdsvis 1,0 og 1,3 % fukt. Det ble ikke korrigert for dette forholdet ved måling eller beregning av frysetemperatur.

Salt og vann ble veid opp ved romtemperatur vha. en Mettler PM 1200 vekt med oppløsning 0.001 g og nøyaktighet 0.005 g.
Løsningstemperatur ble målt med Termocoax termoelement type E med knust is som referansetemperatur. Målepunktet var tilknyttet en HP Agilent datalogger som lagret data hvert tiende sekund. Nøyaktighet (2σ) for temperaturmåling var ± 0.1 K.

Det var ønskelig å finne frysetemperatur for is ved følgende løsningskonsentrasjoner: 5, 10, 15, 20, 25, 30 vekt-% (kg salt/kg løsning). Konsentrasjon ble definert som kg salter pr. kg ferdig løsning. Vektforholdet NaCl og $MgCl_2$ skulle holdes konstant på 70/6 mens konsentrasjonen ble endret ved å variere vannmengden.
En konsentrasjon på 30 % ville gi 55 g NaCl i 140 g vann (28.2 vekt-%). Som vist i Figur 1 ville dette gi uoppløst NaCl i blandingen siden metningspunkt for NaCl i vann ved 20 °C er 35.8 g pr. 100 g vann, dvs. 26.4 vekt-% NaCl.
I stedet for en konsentrasjon på 30 vekt-% ble dette forsøket utført ved 27 vekt-% (26.3 vekt-% NaCl) som var den teoretisk største konsentrasjonen hvor all NaCl var oppløst i vannet.

Eutektisk konsentrasjon for en NaCl-vann løsning er 23.3 %. Siden testene ved 25 % og 27 % begge hadde høyere konsentrasjon ble to tester med NaCl og $MgCl_2$ konsentrasjon på 17.5 % og 22.5 % også utført for å få 6 punkter på grensekurven mellom *umettet* løsning og *is+mettet* løsning. I testene ved 25 og 27 % antas det at blandingen vil kjøles ned til metningslinjen mot *$NaCl{\cdot}2H_2O$* området. Ved videre kjøling antas konsentrasjonen å følge metningslinjen ned til eutektisk NaCl-konsentrasjon. Dette gjelder for en enkeltsaltløsning og forløpet i en tosaltløsning kan være forskjellig fra dette.

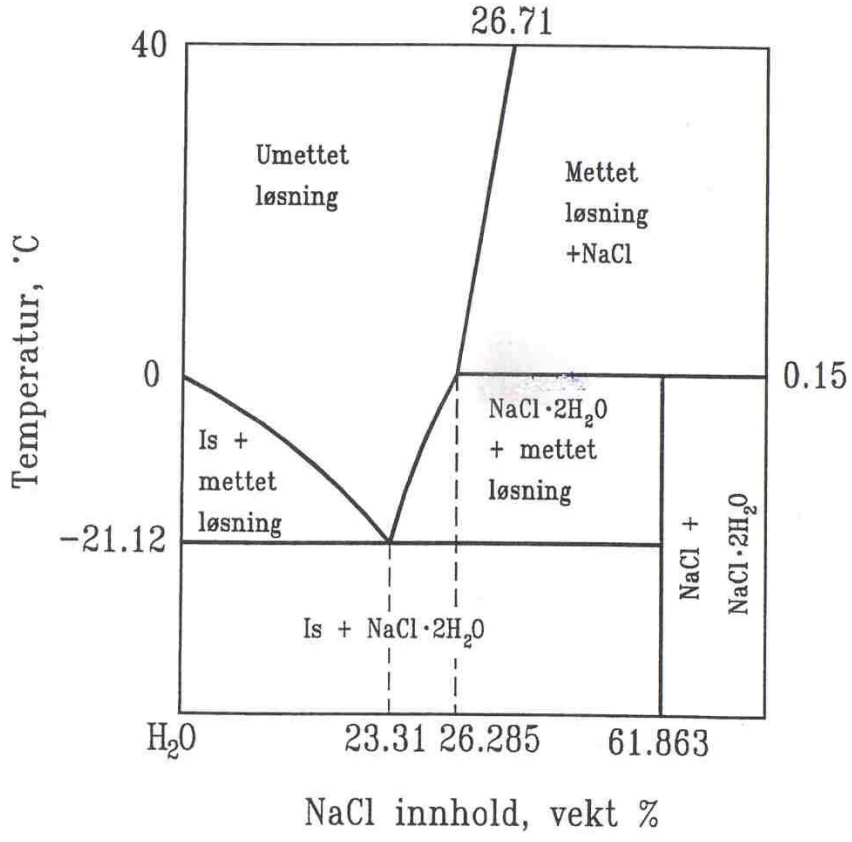

Figur 1: Fasediagram for NaCl-H20 system, (skjematisk, ikke skalert) fra SINTEF (1995)

5 RESULTATER

Nedkjølingsforløp som funksjon av tid for alle målingene er gitt i vedlegg 1.
Tabell 1 viser blandingsforholdet for hvert enkelt forsøk. Vekt-% $MgCl_2$ og NaCl ble definert som vekt av henholdsvis $MgCl_2$ eller NaCl dividert på total vekt. Konsentrasjon ble definert som vekt av $MgCl_2$ og NaCl dividert på total vekt. Total vekt var summen av $MgCl_2$-$6H_20$, NaCl og vann.

Tabell 1. Mengder, blandingsforhold og konsentrasjoner

$MgCl_2$ -$6H_2O$, g	$MgCl_2$, g[1]	NaCl, g	H_2O, g	Total, g[2]	$MgCl_2$, vekt-%	NaCl, vekt-%	H2O, vekt-%	Konsen-trasjon, %
1,752	0,788	9,212	190,080	201,04	0,4	4,6	94,5	5,0
3,504	1,577	18,430	180,140	202,07	0,8	9,1	89,1	9,9
5,266	2,370	27,634	170,007	202,91	1,2	13,6	83,8	14,8
6,161	2,772	32,231	165,087	203,48	1,4	15,8	81,1	17,2
7,027	3,162	36,853	160,031	203,91	1,6	18,1	78,5	19,6
7,895	3,553	41,460	155,115	204,47	1,7	20,3	75,9	22,0
8,781	3,951	46,044	150,03	204,85	1,9	22,5	73,2	24,4
9,52	4,284	50,044	140,01	199,57	2,1	25,1	70,2	27,2

[1]Angitt $MgCl_2$ mengde er ikke veid opp men beregnet som 45 % av oppveid $MgCl_2$-$6H_20$ mengde.
[2] Sum $MgCl_2$-$6H_2O$, NaCl og vann

Det ble observert underkjøling i alle forsøkene og i.h.t standard (vedlegg 3, FIG.3b) ble frysepunktstemperatur, T_{fi}, definert som høyeste temperatur like etter frysestart. Tabell 2 viser målt og beregnet temperatur for isfrysepunkt ved ulike konsentrasjoner. Kolonnen "Underkjøling" viser laveste løsningstempertur før frysing startet.

Tabell 2. Målt og beregnet startfrysetemperatur.

$MgCl_2$, vekt-%	NaCl, vekt-%	H2O, vekt-%	Konsentrasjon, %	Under-kjøling, K	Målt, temperatur, °C	Beregnet temperatur, °C
0,4	4,6	94,5	5,0	0,5	-3,1	-2,9
0,8	9,1	89,1	9,9	0,4	-6,8	-6,6
1,2	13,6	83,8	14,8	0,6	-11,2	-11,3
1,4	15,8	81,1	17,2	0,6	-13,9	-14,0
1,6	18,1	78,5	19,6	0,6	-17,1	-17,0
1,7	20,3	75,9	22,0	0,8	-20,5	-20,4

Tabell 3 viser målt isfrysetemperatur ved konsentrasjoner høyere enn eutektisk konsentrasjon for en NaCl-H_2O løsning. Siden ligningen for startfrysetemperatur kun er gyldig ned til eutektisk NaCl-konsentrasjon (23.3 vekt-%) er det ikke beregnet temperaturer for disse konsentrasjonene.

Tabell 3. Målt startfrysetemperatur.

$MgCl_2$, vekt-%	NaCl, vekt-%	H2O, vekt-%	Start-konsentrasjon, %[1]	Underkjøling, K	Målt temperatur, °C
1,9	22,5	73,2	24,4	3,2	-21,7
2,1	25,1	70,2	27,2	1,5	-22,0

[1] Konsentrasjon ved startfrysepunkt vil avvike fra startkonsentrasjon p.g.a utfelling.

Figur 2 viser sammenligning av målt og beregnet frysepunktstemperatur. Målt underkjøling er angitt med horisontale linjer under hvert målepunkt. Frysetemperatur for de to målingene med startkonsentrasjon 24.4 og 27.2 % er angitt ved eutektisk (23.3 %) NaCl konsentrasjon.

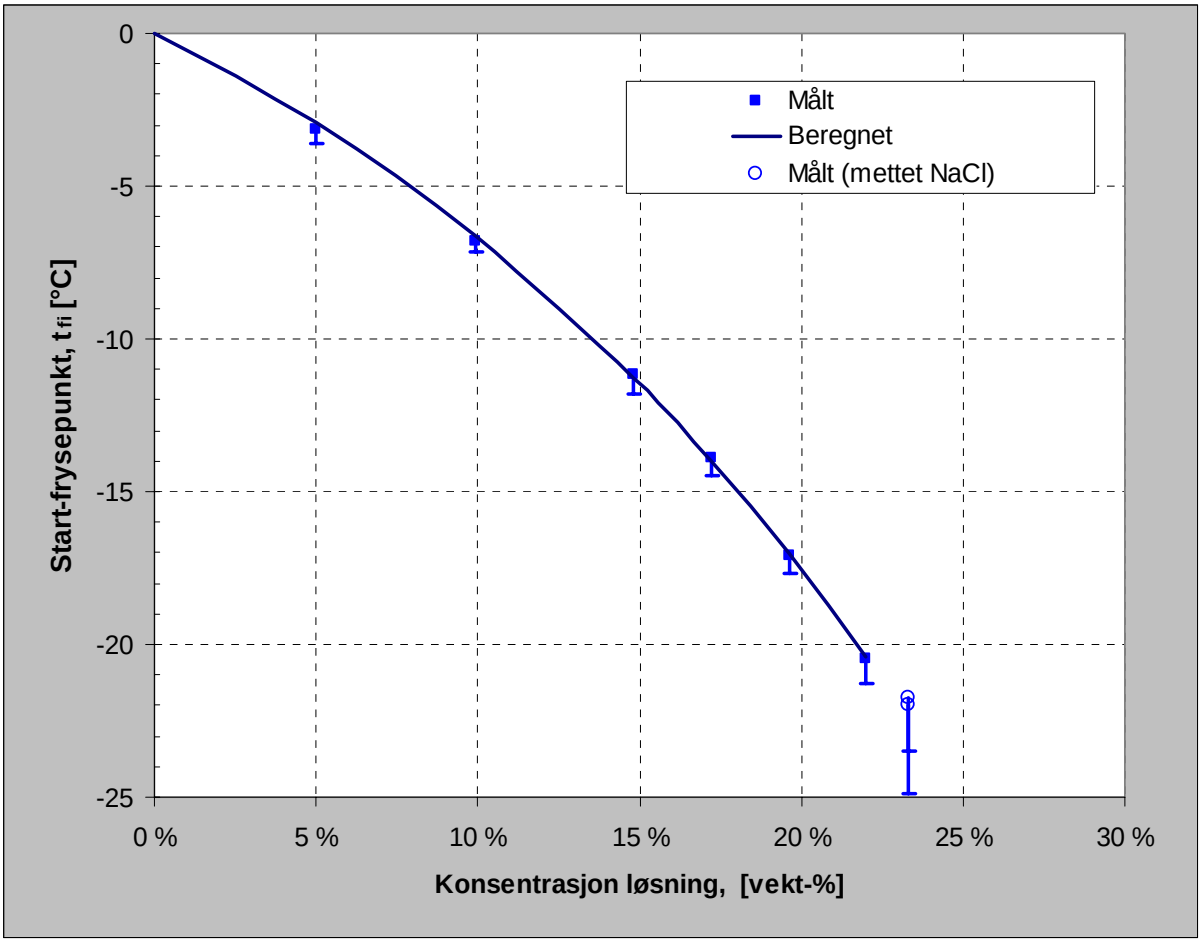

Figur 2. Målt og beregnet starttfrysetemperatur ved ulike konsentrasjoner. Konsentrasjon ved laveste målte temperatur er anslått til 23.3 %.

Standardavvik for målt og beregnet temperatur var 0,13 °C. Største differanse var -0,2 °C.

En sammenligning av isfrysetemperatur som funksjon av konsentrasjon for løsninger med NaCl-H_2O, $MgCl_2$-H_2O og NaCl-$MgCl_2$- H_2O er vist i Figur 3. Beregninger er foretatt vha. av metode beskrevet i kapittel 3.

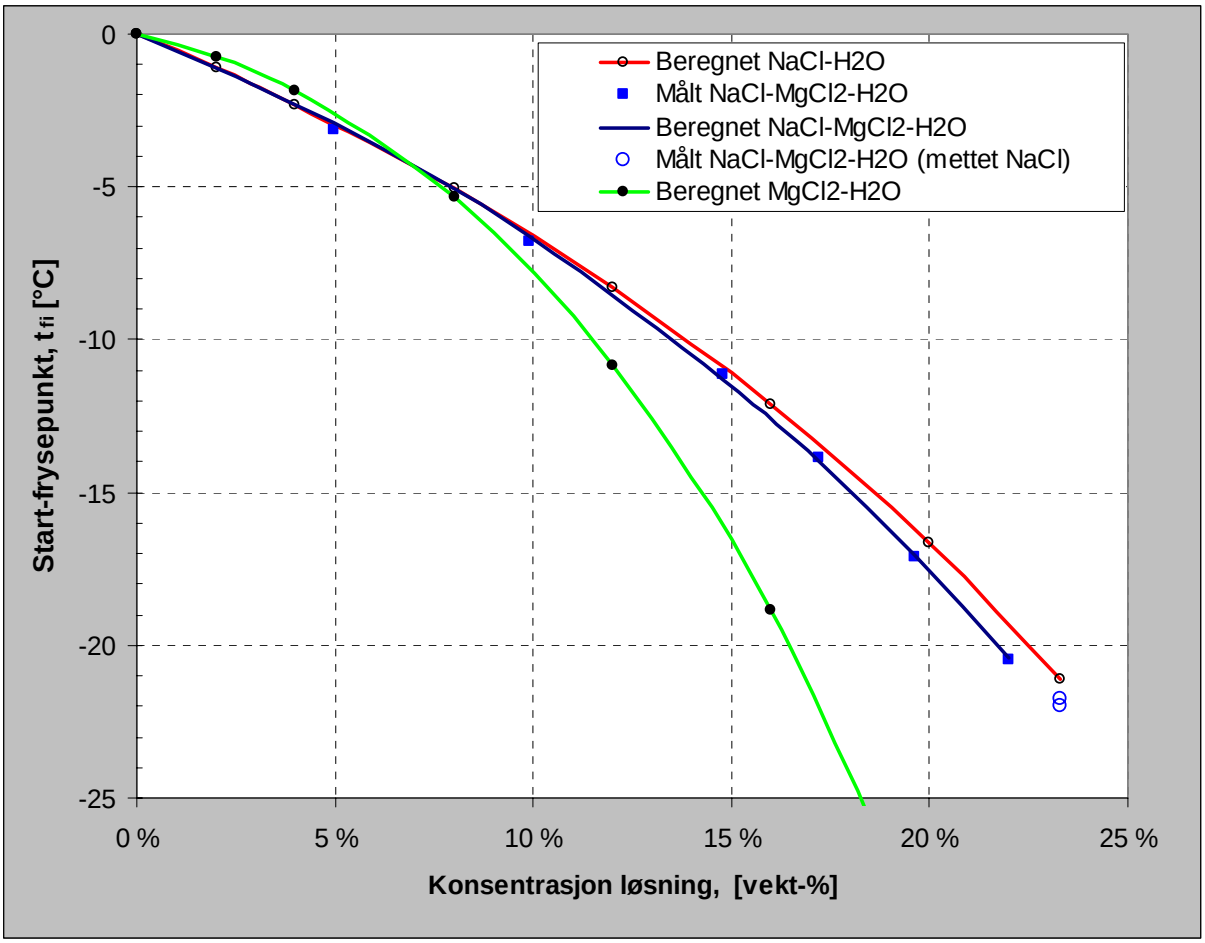

Figur 3. Startfrysetemperatur som funksjon av konsentrasjon for løsninger med NaCl-H_2O, $MgCl_2$-H_2O og NaCl-$MgCl_2$- H_2O. Konsentrasjon ved laveste målte temperatur er anslått til 23.3 %. Beregninger er foretatt vha. av metode beskrevet i vedlegg 2.

Figur 3 kan misforstås dersom en sammenligner en NaCl-H20 og en NaCl-MgCl2- H2O løsning ved samme konsentrasjon. Det kan se ut som om frysepunktstemperaturen kun senkes mindre enn én grad ved å tilsette $MgCl_2$. Men, som eksemplet i Tabell 4 viser vil konsentrasjonen også endres ved tilsetting av $MgCl_2$ i en NaCl-H_2O løsning og frysepunktet blir vesentlig lavere.

Tabell 4 Frysepunktsendring ved å tilsette $MgCl_2$ i en NaCl-H2O løsning.

$MgCl_2$, g	**NaCl, g**	**H_2O, g**	**Total, g**	**$MgCl_2$, vekt-%**	**NaCl, vekt-%**	**H2O, vekt-%**	**Konsen-trasjon, %**	**Beregnet frysetemperatur, °C**
0	20	80	100	0	20	80	20,0	-16,7
1,714[1]	20	80	101,714	1,7	19,7	78,2	21,3	-19,4

[1] 6/70 av opprinnelig NaCl mengde.

6 KONKLUSJON

For en vannløsning med vektforholdet NaCl-$MgCl_2$ på 70/6 er temperatur ved frysestart målt og funnet i overensstemmelse med data i litteraturen.

7 REFERANSER

Dubois. M (1997) *The H_2O-NaCl-$MgCl_2$ ternary phase diagram with special application to fluid inclusion studies*. Economic geology Vol. 92, 1997, pp. 114-119

Melinder, Åke (1997) *Termofysikaliska egenskaper för köldbärarvätskor*.

SINTEF (1995) rapport STF11 F95008. *Bruk av saltløsninger til vegvedlikehold*.

Spencer, R. J., Møller, N. et Weare, J. H. (1990): *The prediction of mineral solubilities in natural waters: A chemical equilibrium model for the Na-K-Ca-Mg-Cl-SO_4-H_2O system at temperatures below 25°C*. Geochim. Cosmochim. Acta, 54, 575-590

8 VEDLEGG

8.1 VEDLEGG 1, MÅLT TEMPERATUR-TID FORLØP.

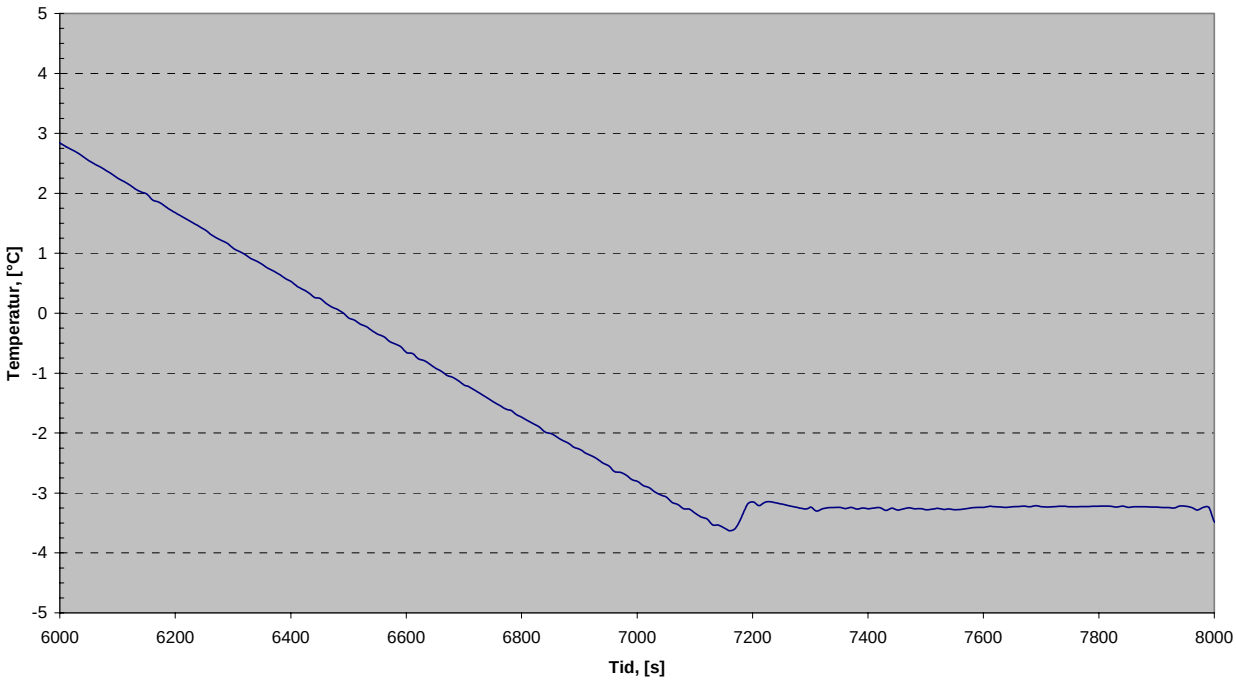

5 % løsning

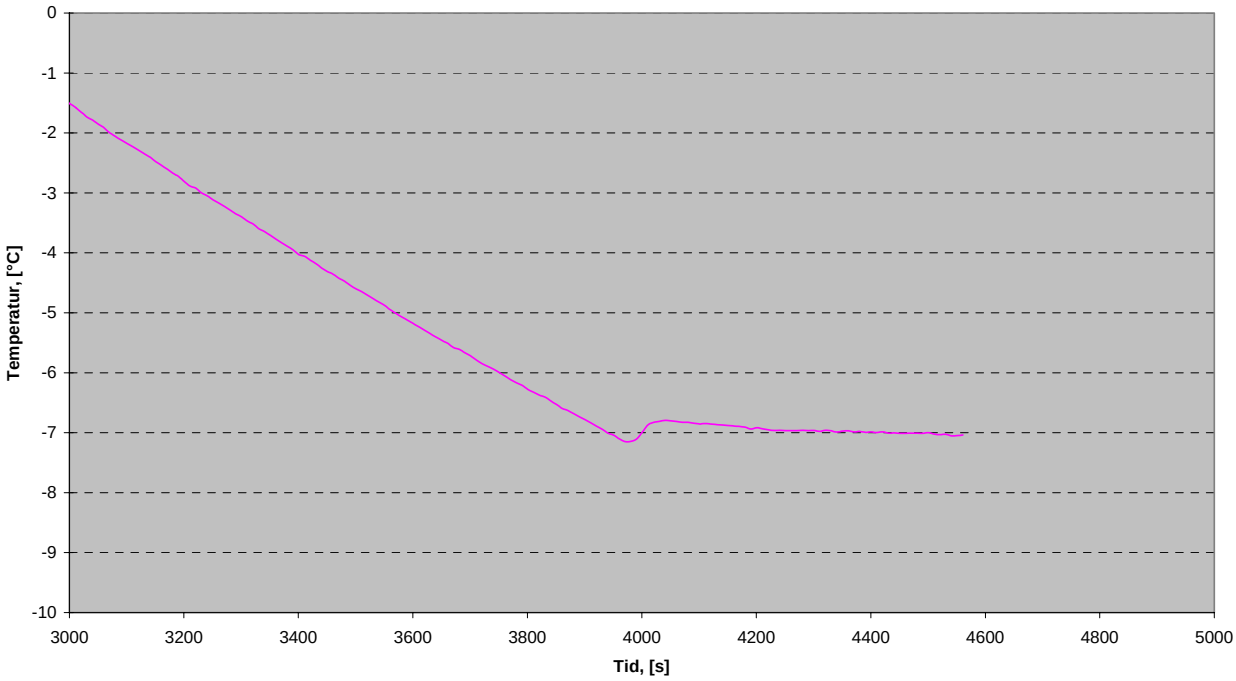

10 % løsning

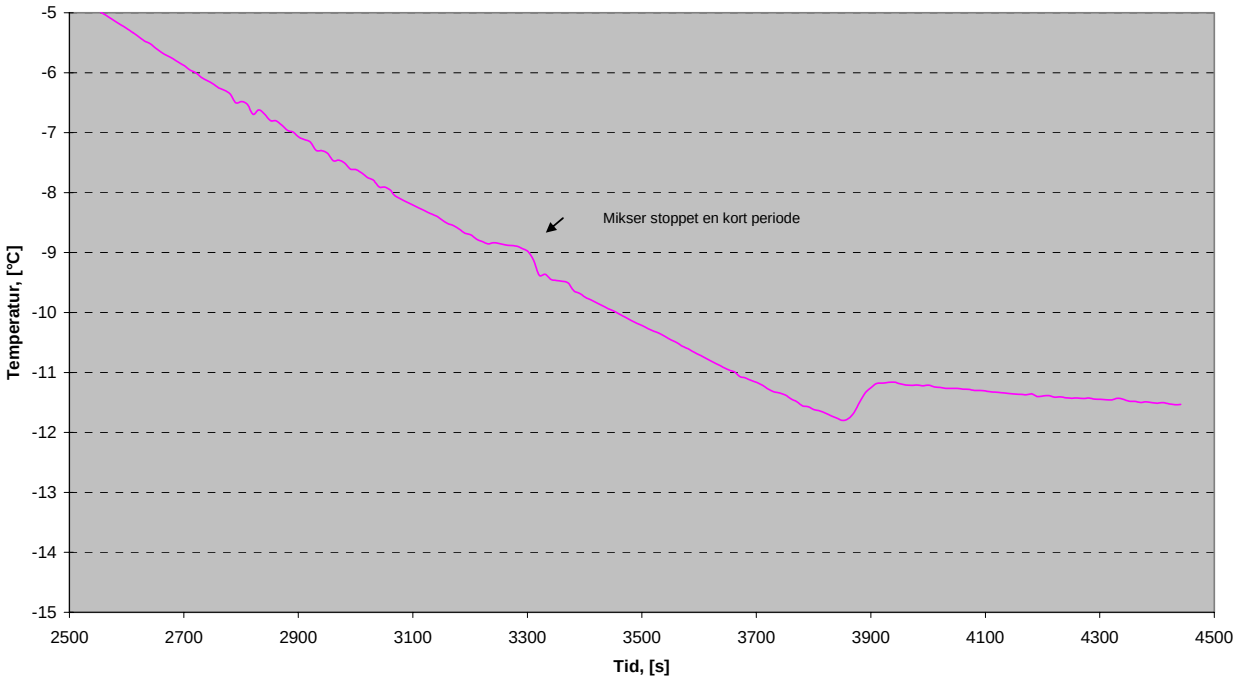

15 % løsning

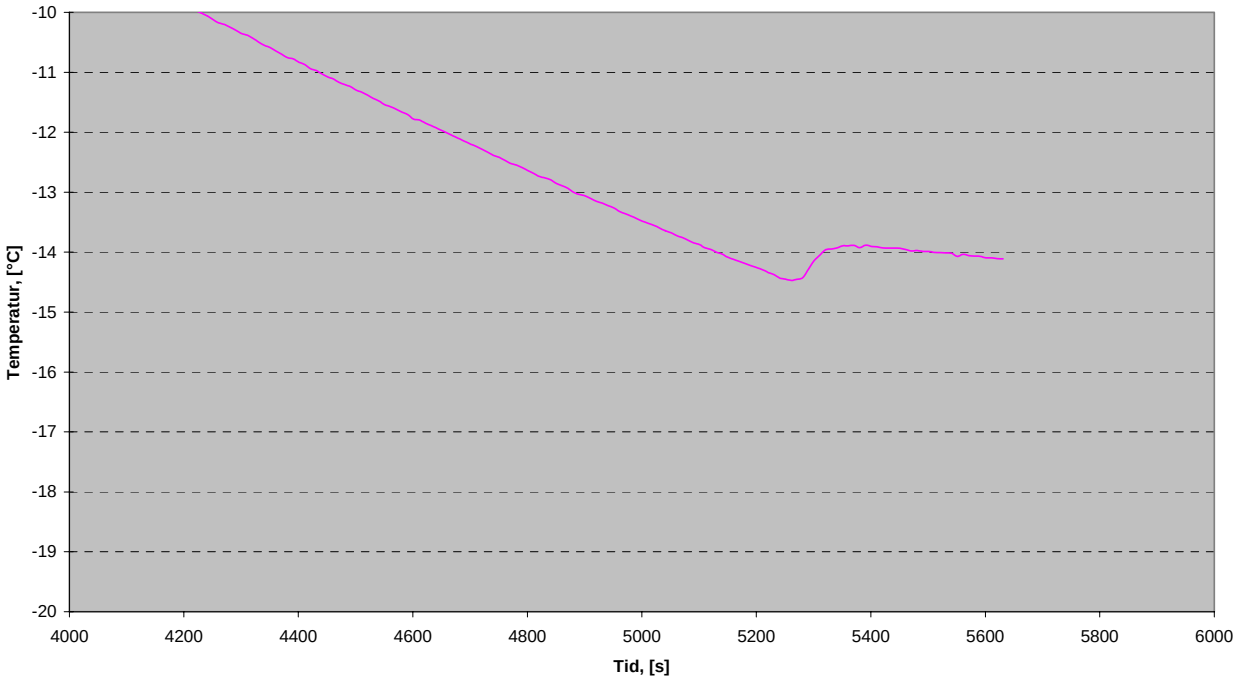

17,5 % løsning

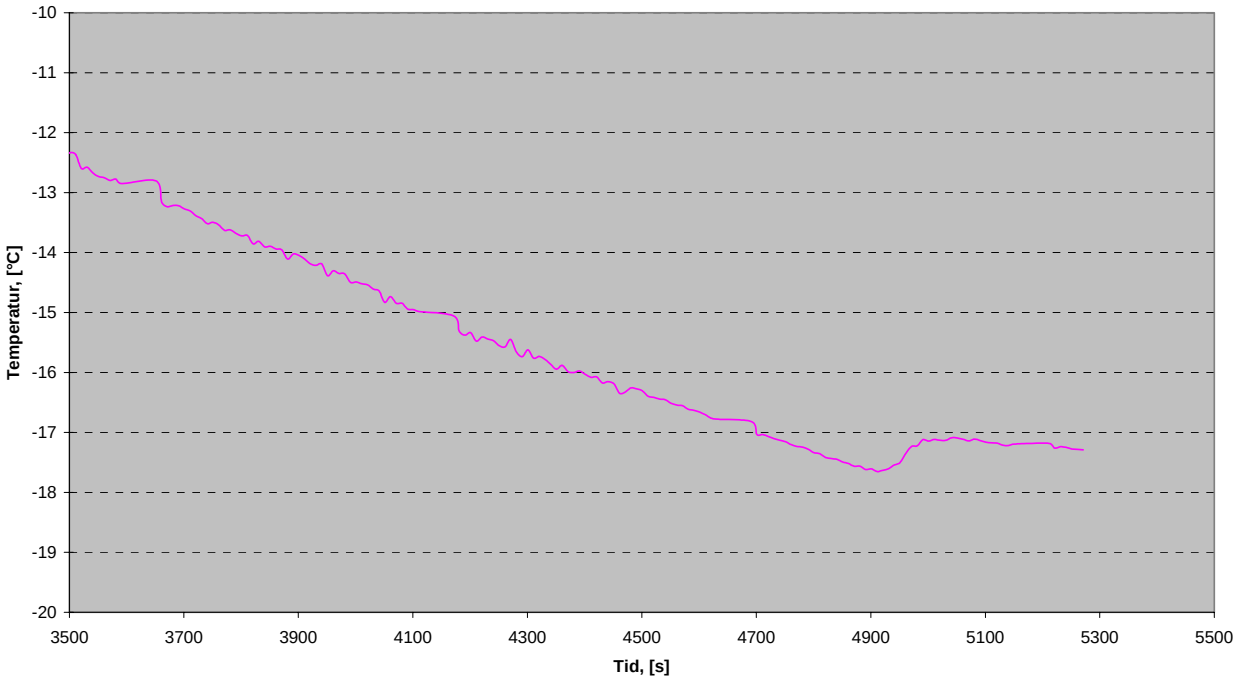

20 % løsning

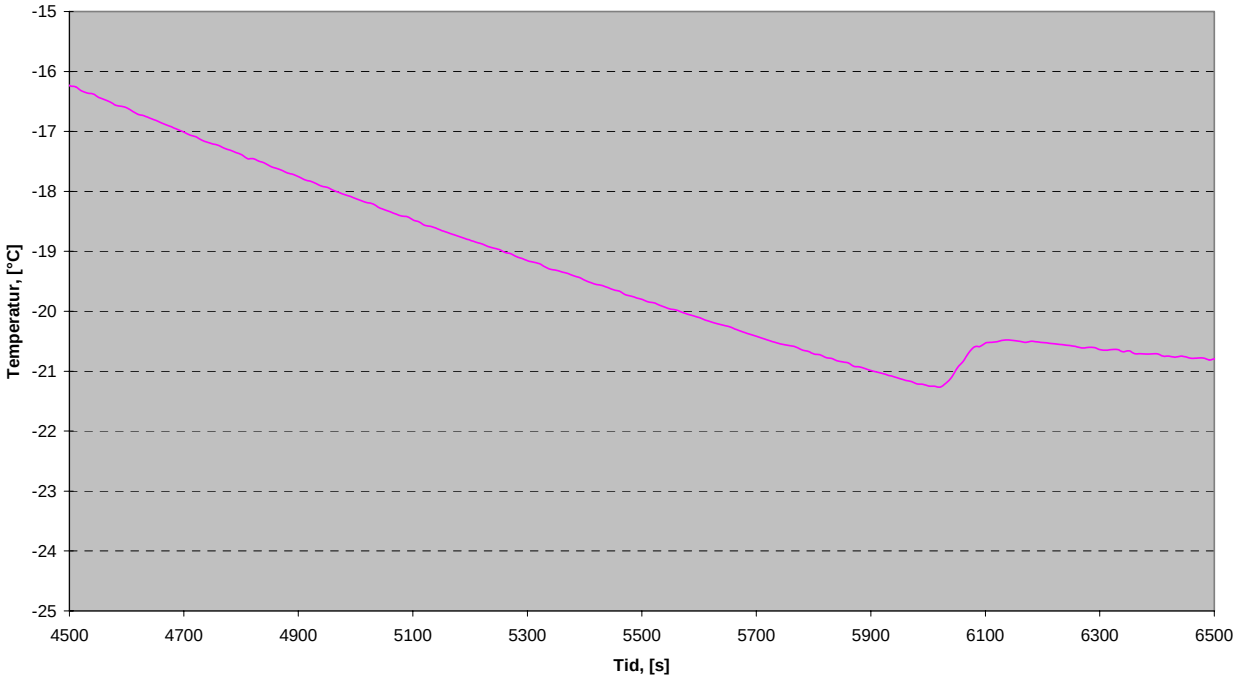

22,5 % løsning

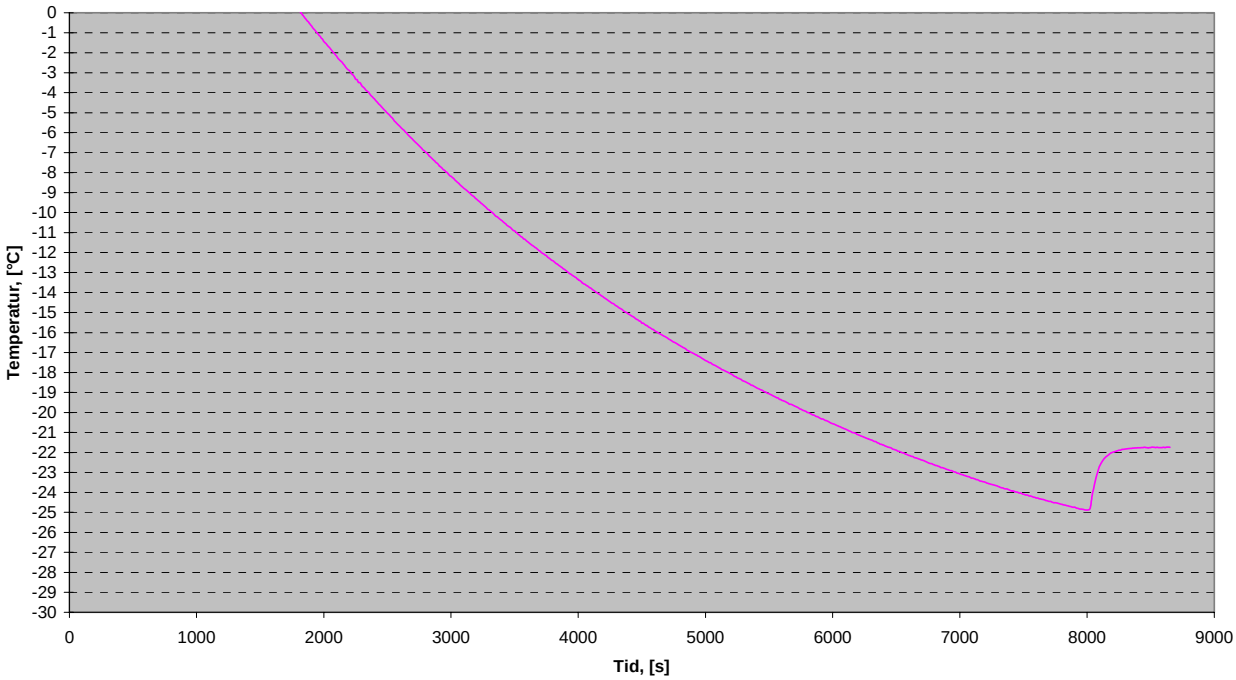

25 % løsning

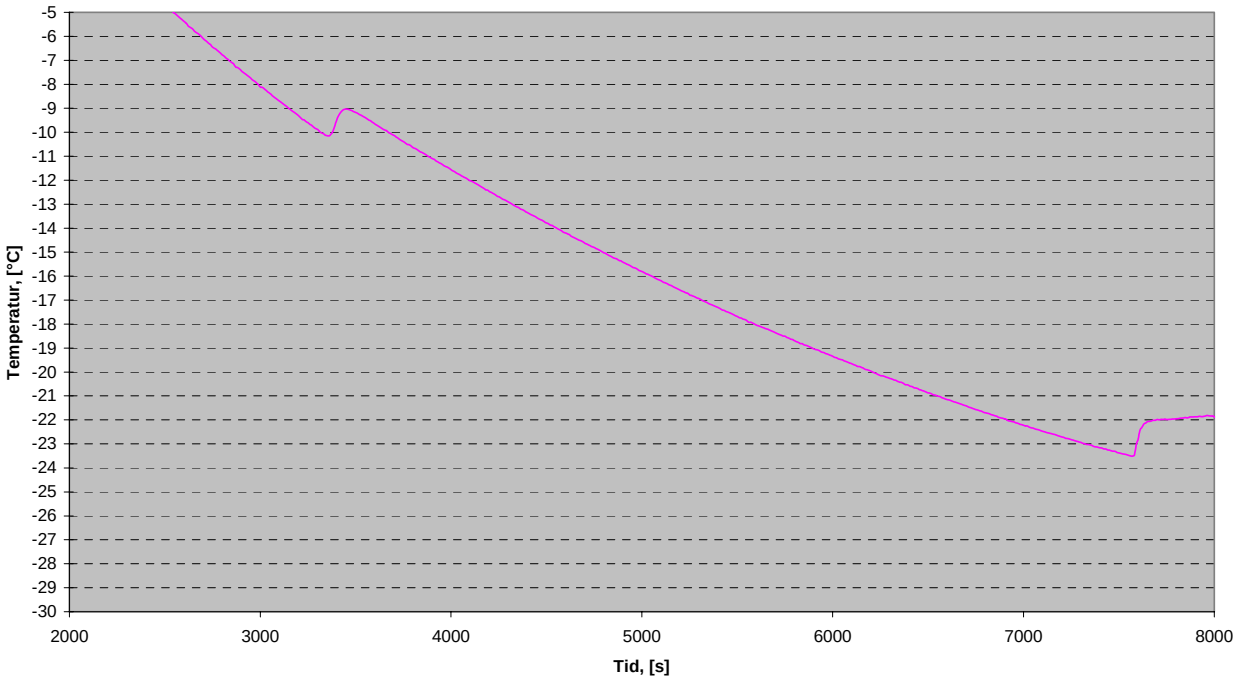

27 % løsning

8.2 VEDLEGG 2, LITTERATURSØK

Economic Geology
Vol. 92, 1997, pp. 114–119

THE H_2O-NaCl-$MgCl_2$ TERNARY PHASE DIAGRAM WITH SPECIAL APPLICATION TO FLUID INCLUSION STUDIES

M. DUBOIS

Université des Sciences et Technologies de Lille, URA 719, Sciences de la Terre, 59655 Villeneuve d'Ascq Cedex, France

AND C. MARIGNAC

E.N.M.I.M., Parc de Saurupt, 54000 Nancy, France, and C.R.P.G., Centre National de la Recherche Scientifique, 15 rue Notre-Dame des Pauvres, BP 20, 54501 Vandœuvre-les-Nancy, France

Introduction

Determination of the compositions of fluid inclusions requires knowledge of the system chemistry and the appropriate phase equilibria for that system. The standard approach consists of identifying the major components, using the eutectic temperature and determining the major solute concentrations using solid phase melting temperatures. The phase rule implies that in an n component system, the $n - 1$ phase transition temperatures must be known. The melting temperature of ice ($T_{m_{ice}}$ in low-salinity fluids) or salt ($T_{m_{salt}}$ in saturated solutions) is often easily measured, and this temperature can be interpreted in terms of composition in a simple binary system such as H_2O-NaCl (wt % NaCl equiv). However, Ramboz (1980) and Haynes (1985) have shown that by using a sequential freezing method, other phases (salt hydrates, such as hydrohalite or gas clathrates) can be identified and their melting temperatures measured. The bulk composition can, therefore, be estimated graphically using a more complicated phase diagram, generally ternary (Crawford et al., 1979; Haynes, 1985; Vanko et al., 1988).

Many ternary systems have been used in fluid inclusion studies, including the more common salts such as NaCl (which is often the dominant species), KCl, and $CaCl_2$; other species such as LiCl may also be present (Aïssa et al., 1987; Cathelineau et al., 1994). The solubility relations in the system H_2O-NaCl-KCl were studied by Sterner et al. (1988). The system H_2O-NaCl-$CaCl_2$ was studied with special application to fluid inclusion studies (Vanko et al., 1988; Oakes et al., 1990; Williams-Jones and Samson, 1990) in order to model geologic fluids in Ca-rich systems.

Fluid inclusions in barite in a hydrothermal chimney from the Lau basin have a eutectic temperature of $-35° \pm 1°C$, consistent with a fluid composition belonging to the H_2O-NaCl-$MgCl_2$ system. This occurrence prompted us to look for data concerning this system and to reconstruct the solubility relations in the corresponding ternary phase diagram.

Reconstruction of the H_2O-NaCl-$MgCl_2$ System

The reconstruction of the H_2O-NaCl-$MgCl_2$ ternary phase diagram requires the knowledge of the stability fields of ice, hydrohalite, the hydrates of $MgCl_2$, halite, and liquid.

Our study particularly focused on the ice-melting area, which is a three-dimensional surface in m_{NaCl}-m_{MgCl_2}-temperature space (m_{NaCl}-m_{MgCl_2} are the NaCl and $MgCl_2$ m, respectively). This surface is limited by four three-phase curves under vapor pressure: two ice-melting curves of the H_2O-NaCl and H_2O-$MgCl_2$ subsystems and two ice-melting cotectic curves of the ternary system.

H_2O-NaCl subsystem

The H_2O-NaCl system is well studied and is characterized by the presence of an intermediate compound, hydrohalite ($NaCl \cdot 2H_2O$), which is stable between $-21.2°C$ (eutectic temperature) and $+0.1°C$. The experimental points along the ice-liquid-vapor curve are from Rüdorff (1861), Rodebush (1918), Khitrova (1954), Mun and Darer (1957), Stephen and Stephen (1963), Gibbard and Gossmann (1974), Potter et al. (1978), and Hall et al. (1988). The equation of Sterner et al. (1988) was used for drawing the solubility curves of hydrohalite and halite in water.

H_2O-$MgCl_2$ subsystem

The binary H_2O-$MgCl_2$ subsystem shows a eutectic temperature of $-33.6°C$ corresponding to a composition of 20.6 wt percent $MgCl_2$ (2.79 m; Wolff et al., 1986; Fig. 1). It is complicated by the presence of five intermediate hydrates, containing 12 (referred as MG12), 8 (MG 8), 6 (bischoffite, MG6), 4 (MG4), and 2 (MG2) water molecules, respectively (Dupuis, 1958; Spencer et al., 1990; Spencer and Lowenstein, 1992; Fig. 1). The presence of two polymorphic species of MG8 (so-called a and b) has been also described. A complete thermodynamic model was given by Spencer and Lowenstein (1992) along with the properties of each invariant point; however, the MG6-MG4 peritectic reported at 9.48 m (47.44 wt %) is doubtful according to these authors. Actually, Spencer and Lowenstein (1992) give a peritectic composition of 9.48 m (47.44 wt %), which does not respect the thermodynamic constraint that the disappearing phase composition MG6 (9.26 m, 46.86 wt %) must lie between the appearing phase composition MG4 (13.89 m, 56.94 wt %) and the liquid composition, according to the reaction MG6 + liquid → MG4 + liquid.

The ice-liquid-vapor curve was fitted using the data of Prutton and Tower (1932), Mun and Darer (1957), Linke (1958), Gibbard and Gossmann (1974), and Wolff et al. (1986).

H_2O-NaCl-$MgCl_2$ ternary

The H_2O-NaCl-$MgCl_2$ ternary system is characterized by a eutectic temperature of $-35°C$. The corresponding composition is 1.105 m NaCl (4.97 wt %) and 2.484 m $MgCl_2$ (18.18 wt %; Spencer et al., 1990). Note that the eutectic composition that is generally cited (1.56 wt % NaCl, 22.71 wt % $MgCl_2$) was obtained by Luzhnaja and Vereshtchetina (1946) in a study dealing with the quaternary system H_2O-NaCl-$MgCl_2$-$CaCl_2$. Their values are inconsistent for reasons already discussed by Spencer et al. (1990), who have noted

0361-0128/97/1909/114-6$6.00

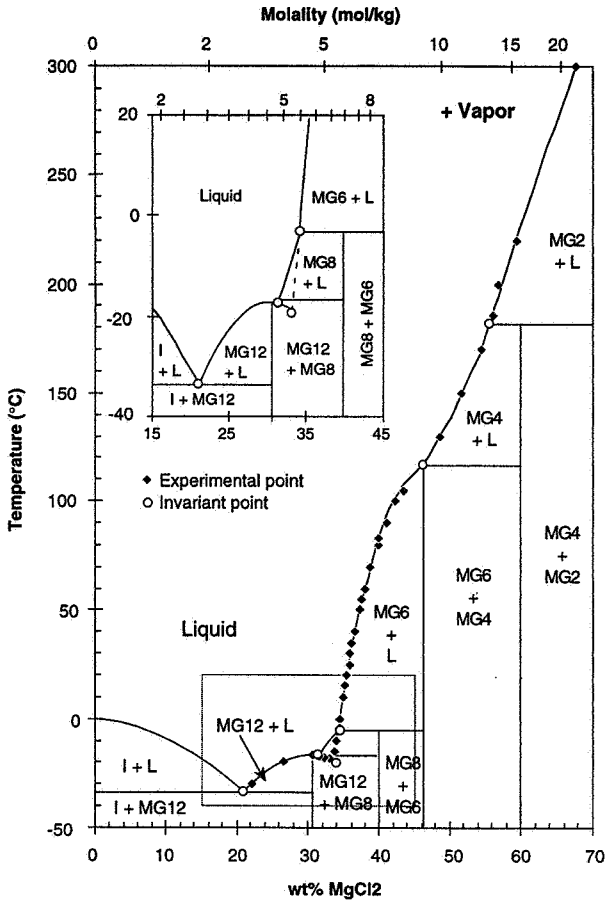

FIG. 1. General x-T representation of the H_2O-$MgCl_2$ system. The inset is a detailed representation of the stability field of $MgCl_2 \cdot 8H_2O$. Abbreviations: I = ice, L = liquid, MGx = $MgCl_2$ hydrate, including x water molecules. Ice-liquid-vapor curve is from Prutton and Tower (1932), Mun and Darer (1957), Linke (1958), Gibbard and Gossmann (1974), and Wolff et al. (1986). Data on the solid-liquid-vapor curves are from Takegami (1921), Keitel (1923), Kournakov and Zemcuznyj (1924), Dupuis (1958), and Linke (1958).

that the data obtained from many muticomponent systems have low accuracy in the relevant subsystems.

The ice-liquid-vapor surface shown in Figure 2 was reconstructed using the data available along the cotectic ice + hydrohalite + liquid and ice + MG12 + liquid curves (Spencer et al., 1990) and the ice-melting temperatures of Mun and Darer (1957) and Gibbard and Gossmann (1974). In order to simplify the calculation, a second-order polynomial fit was made with compositions expressed in molality, in a cartesian coordinate system. The temperature (°C) was fitted as function of composition according to:

$$T\,(°C) = \sum_{i=0}^{2} \sum_{j=0}^{2} a_{ij}\, m_{NaCl}^{i}\, m_{MgCl_2}^{j} \qquad (1)$$

The fitting coefficients were calculated using a general least squares method (Johnson and Wichem, 1982). However, four constraints were applied to the fit according to a method used by Dubois et al. (1993): the ternary eutectic point, the eutectic points of the two subsystems, and the ice-melting temperature at 0°C for pure water ($m_{NaCl} = m_{MgCl_2} = 0$, which implies

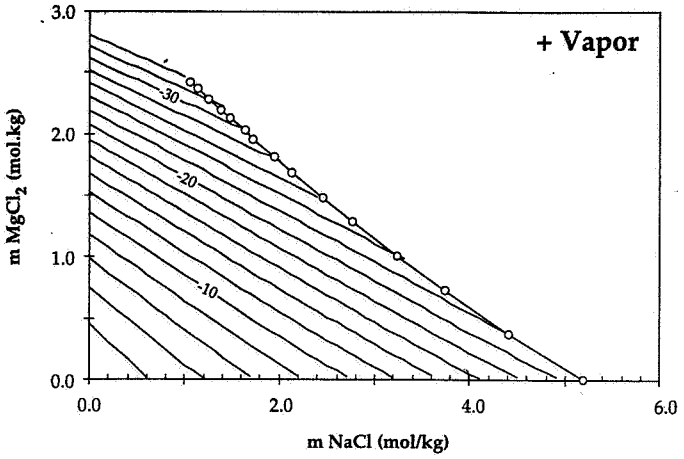

FIG. 2. An m_{NaCl}-m_{MgCl_2} diagram representing the isotherms (in 2°C intervals) of the ice-liquid-vapor surface in the H_2O-NaCl-$MgCl_2$ system, using equation (1) and the coefficients given in Table 1.

that $a_{00} = 0$). The calculated a_{ij} coefficients are listed in Table 1. Figure 2 gives a representation of the isotherms of the ice-liquid-vapor surface with a 2°C step.

The reliability of the fit is shown in Figure 3 and in Table 2. Figure 3A and B corresponds to the boundary conditions of the ice-liquid-vapor surface for the $m_{MgCl_2} = 0$ and $m_{NaCl} = 0$ subsystems. The fit along the ice-liquid-vapor curve of the H_2O-NaCl subsystem appears to be excellent (Fig. 3A), whereas it differs by ±0.5°C along the ice-liquid-vapor curve of the H_2O-$MgCl_2$ subsystem (Fig. 3B). Table 2 gives a comparison between the experimental values and the calculated ones; errors are less then 0.2°C.

A convenient triangular representation of the phase diagram is given in Figure 4 by converting molalities to wt percent (wt %). The isotherms of the ice + liquid surface were drawn with a 2°C step. Additional data for the halite dissolution surface are represented as isotherms to 200°C.

Application to Fluid Inclusion Studies

In the common case of low-salinity NaCl-$MgCl_2$-H_2O solutions where NaCl predominates, the eutectic is marked by the melting of the Mg-bearing phase (MG12), recognizable by the granulation of the liquid (Davies et al., 1990). The corresponding temperature is theoretically −35°C, but in high Mg content solutions lower eutectic temperatures can be measured, corresponding to a metastable equilibrium between MG8 or MG6 and ice (Spencer et al., 1990). Between the eutectic temperature and a temperature lower than −21.2°C, hydrohalite coexists with ice; hydrohalite can be identified as rounded birefringent solids (Davies et al., 1990). Above the hydrohalite-melting temperature, ice is stable until

TABLE 1. Fitting Coefficients of Equation 1

i/j	0	1	2
0	0.0000	−2.8438 ± 0.0033	−3.2935 ± 0.0012
1	−3.1203 ± 0.0010	−2.8430 ± 0.0104	0.4518 ± 0.0033
2	−0.1813 ± 0.0002	0.1581 ± 0.0025	0.0396 ± 0.0015

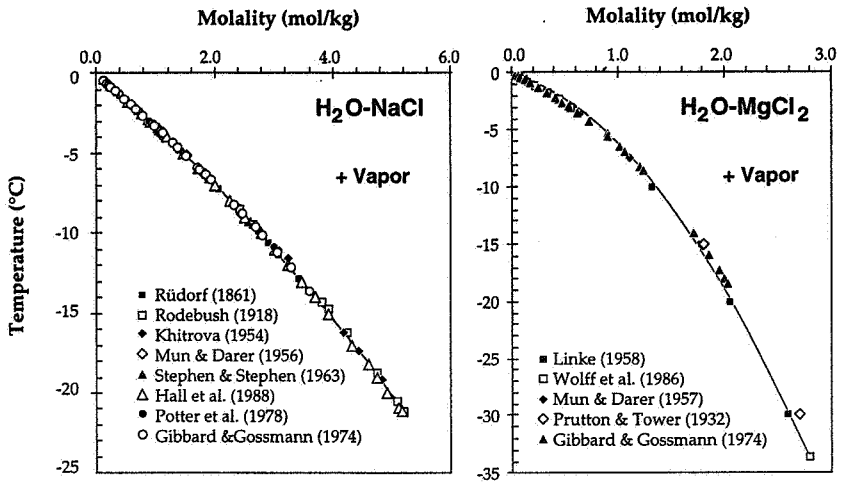

FIG. 3. Reliability of the fit along the ice-liquid-vapor curves of the subsystems (A) H_2O-NaCl, and (B) H_2O-$MgCl_2$.

TABLE 2. Comparison between Experimental and Calculated Temperatures

Reference	m_{NaCl}	m_{MgCl_2}	T_{exp}	T_{calc}	ΔT
[1]	0.382	1.418	−12.650	−13.021	0.371
	0.755	1.045	−10.650	−10.779	0.129
	1.135	0.665	−8.720	−8.882	0.162
	1.464	0.336	−7.330	−7.486	0.156
	0.208	0.902	−6.500	−6.350	−0.150
	0.461	0.649	−5.700	−5.448	−0.252
	0.681	0.429	−4.850	−4.774	−0.076
	0.901	0.209	−4.240	−4.186	−0.054
	0.135	0.505	−3.200	−2.876	−0.324
	0.261	0.379	−2.850	−2.638	−0.212
	0.392	0.248	−2.550	−2.418	−0.132
	0.513	0.127	−2.280	−2.239	−0.041
[2]	0.893	0.893	−9.666	−9.908	0.242
	0.673	0.673	−6.709	−6.684	−0.025
	0.448	0.449	−4.118	−3.890	−0.228
	0.308	0.308	−2.964	−2.418	−0.546
	0.212	0.212	−1.808	−1.545	−0.263
	0.122	0.122	−1.018	−0.822	−0.195
	0.070	0.070	−0.579	−0.447	−0.132
	0.038	0.038	−0.319	−0.237	−0.082
	1.487	0.418	−8.111	−8.288	0.177
	0.985	0.277	−5.041	−4.981	−0.061
	0.561	0.157	−2.742	−2.572	−0.169
	0.410	0.115	−1.990	−1.811	−0.178
	0.272	0.076	−1.306	−1.156	−0.150
	0.153	0.043	−0.731	−0.627	−0.103
	0.088	0.025	−0.425	−0.355	−0.070
	0.053	0.015	−0.257	−0.211	−0.047
	2.088	0.231	−9.090	−9.291	0.201
	1.628	0.180	−6.855	−6.912	−0.057
	1.081	0.120	−4.387	−4.309	−0.708
	0.665	0.074	−2.644	−2.516	−0.127
	0.365	0.040	−1.439	−1.325	−0.114
	0.202	0.022	−0.795	−0.714	−0.081
	0.101	0.011	−0.405	−0.353	−0.052

m_{NaCl} and m_{MgCl_2} refer to the respective NaCl and $MgCl_2$ molalities (moles · kg^{-1}), T_{exp} (°C) = the experimental temperature (from references 1 and 2), T_{calc} (°C) = the temperature calculated using equation 1; ΔT (°C) = the difference between experimental and calculated temperatures

References: [1] = Mun and Darer (1957), [2] = Gibbard and Gossman (1974)

it melts at the ice-melting temperature. The hydrohalite-melting temperature gives a point along the ice + hydrohalite + liquid cotectic, and the intersection between the tie line joining that point and the representative point of pure H_2O with the ice-melting temperature isotherm, gives the bulk composition of the solution.

Application to the Hydrothermal Fluids from the Lau Basin (Pacific Ocean)

In the Lau basin, Valu Fa Ridge is a modern back-arc volcanic ridge with three major hydrothermal fields (Fouquet et al., 1991, 1993). From the southernmost Hine Hina field, an inactive chimney composed of sphalerite, marcasite, barite, and chalcopyrite was selected for a fluid inclusion study. In chimney NL 16-02, barite is a late mineral, with well-individualized euhedral crystals, up to 1 cm in length.

Petrographic observation revealed the presence of two fluid inclusion types in barite. The first type is scattered within the barite crystals, mostly isolated or distributed in small clusters but in every case associated with pyrite inclusions. Their mode of occurrence is typically primary using the criteria of Roedder (1979). They are of large size (about 50 μm), allowing an easy observation of phase transition succession. Their geometric form is more or less complex and they contain two phases (liquid and vapor) at room temperature. The second type is distributed along well-defined fractures and consists of small (5–10 μm) two-phase (liquid + vapor) fluid inclusions.

Microthermometric observation was carried out on both types, using a U.S. Geological Survey-type heating and freezing stage calibrated with synthetic fluid inclusions (pure water: ice-melting temperature of 0.0°C and critical homogenization temperature of 374.1°C; pure CO_2 water inclusions: CO_2-melting temperature of −56.6°C). The wafers were prepared so as to prevent leakage of the fluid inclusion in the barite.

The eutectic temperature, ice-melting temperature, and hydrohalite-melting temperature were systematically noted. In type I fluid inclusions, the eutectic temperature is systematically close to −35°C, suggesting the presence of NaCl and

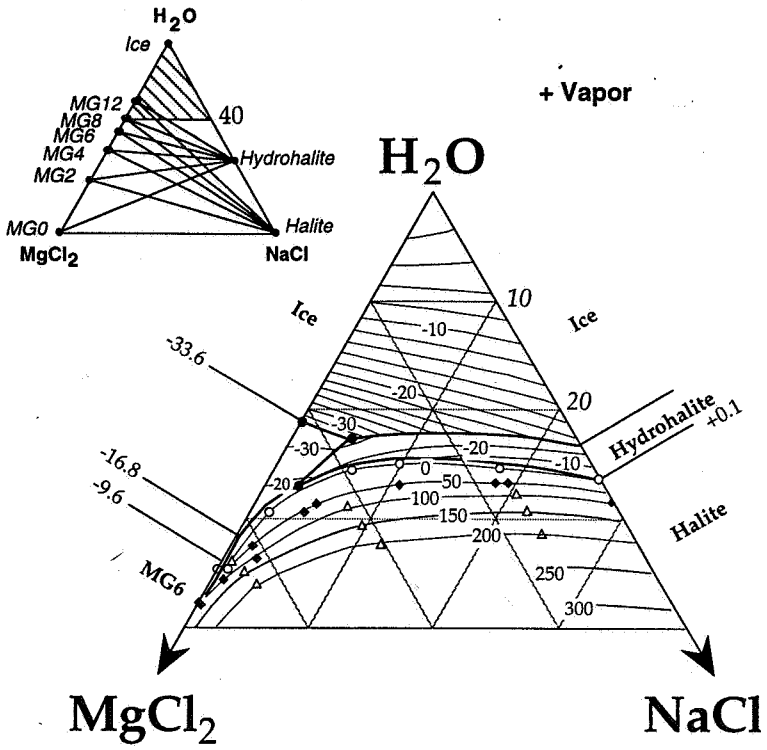

FIG. 4. Ternary representation of the H_2O-NaCl-$MgCl_2$ phase diagram. Isotherm references: 0°C (open circles) from Kournakov and Zemcuznyj (1924), 50°C (black diamonds) from Keitel (1923), and 100° to 200°C (open triangles) from Akhumov and Vassiliev (1933).

$MgCl_2$ as dominating salt species. Ice melts between −2.6° and −1.8°C, with a well-defined mode at −2.3°C (Fig. 5). In these inclusions, the technique of isolating the last ice crystal and its regrowth by applying a cooling event (Haynes, 1985) allows the observation of the freezing of the nonicy part of the inclusion. In this part, salts are concentrated because they do not enter the ice lattice. First melting of the nonicy part is observed at −35°C, leading to the presence of rounded refringent solids identified as hydrohalite. The melting of hydrohalite was observed in the range −25.2° to −22.2°C. T_h measurements are clustered between 175° and 225°C (Fig. 5) and indicate a temperature decrease during barite precipitation (Fouquet et al., 1994; Marignac et al., 1995). In type II inclusions, the eutectic temperatures of −35° ± 1°C were also recorded, but the small size of the inclusions prevented the observation of hydrate melting.

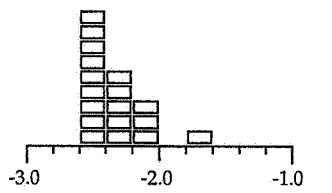

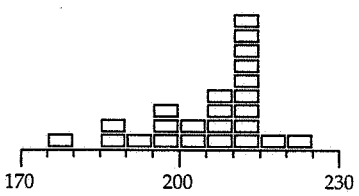

FIG. 5. Histograms of the microthermometric measurements (°C) in primary fluid inclusions in sample NL 16-02 (Lau basin).

Using the two-phase transition temperatures and the assumption that the type I fluid inclusions belong to the H_2O-NaCl-$MgCl_2$ system, the ternary composition was determined and compared to seawater composition. Seawater composition was modeled in the H_2O-NaCl-$MgCl_2$ system; indeed, magnesium is the second most abundant cationic species in seawater (Chester, 1990). The seawater composition was plotted using the melting temperatures of hydrohalite (−22.9°C; Nelson and Thompson, 1954) and ice (−1.921°C; Fujino et al., 1974).

These compositions are shown in Figure 6. The representative points of fluid inclusion compositions appear to differ from the seawater composition by being apparently enriched in $MgCl_2$. The trend shown by fluid compositions may represent a mixing process between seawater and a hydrothermal end member. This end member is characterized by a higher

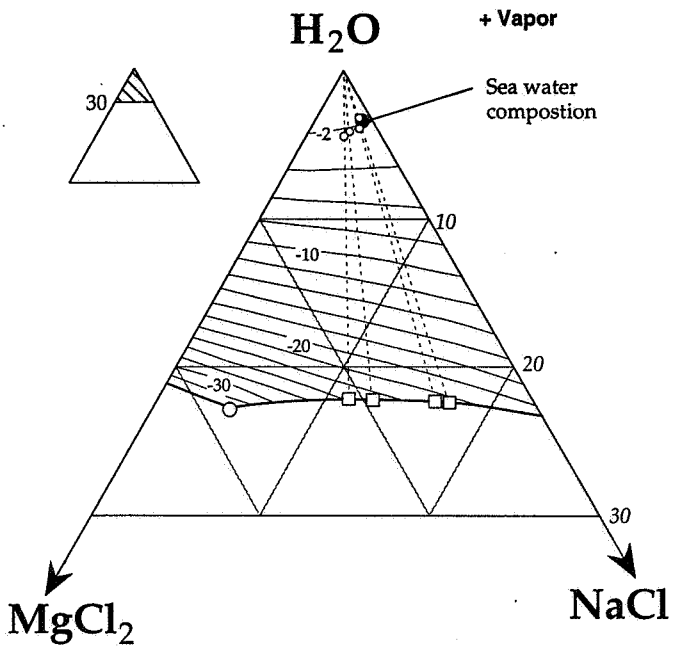

FIG. 6. Plotted compositions of the fluid inclusions in barite from sample NL 16-02 (Lau basin) compared to that of seawater.

salinity and a relative enrichment in magnesium and is interpreted as representing evolved seawater (already depleted in the sulfate component), having undergone boiling to some extent (Marignac et al., 1995).

Conclusions

The H_2O-NaCl-$MgCl_2$ phase diagram is potentially useful for interpreting fluid inclusion data of magnesium-bearing fluids. Such fluids are likely to be observed in several environments. Magnesium is a major component of seawater and, as demonstrated by the fluids from the Lau basin, limited penetration of seawater in the oceanic crust is able to produce fluids enriched in magnesium relative to seawater.

Moreover, intense evaporation of seawater produces water dominated by Na-Mg-Cl, whereas Ca is preferentially removed during precipitation of calcite and gypsum (Hanor, 1994). Such brines can infiltrate down and consequently modify the fluid composition in the underlying sediments by Mg enrichment. Moreover, as shown by Valori et al. (1992) in the Larderello geothermal field, leaching of evaporitic deposits is likely to produce Mg-enriched fluids, evidenced by the presence of fluid inclusions with eutectic temperatures close to −35°C.

In studies dealing with evaporitic environments, the generated Mg-rich fluids may be modeled with the H_2O-NaCl-$MgCl_2$ system, using the ternary diagram developed in the present study. However, caution should be taken for fluids with salinities higher than about 350 to 400 g l^{-1}, where waters produced by seawater evaporation are highly enriched in SO_4^{2-} (Hanor, 1994), which is likely to modify the phase relations.

Acknowledgments

This work was supported by the Programme National d'Etude de l'Hydrothermalisme Océanique program. We would like to thank Y. Fouquet for providing samples, J. Dubessy, B. Gérard, and C. Ramboz for fruitful discussions, and an *Economic Geology* reviewer for helpful comments.

January 17, 1994; December 19, 1995

REFERENCES

Aïssa, M., Marignac, C., and Weisbrod, A., 1987, Caractéristique s chimiques et thermodynamiques des circulations hydrothermales du site d'Echassières: Géologie de la France, v. 2–3, p. 335–350.

Akhumov, E.I., and Vassiliev, B.B., 1933, The technological calculations for the equilibrium of the chlorides of potassium, sodium and magnesium in water at high temperature: Institute of Applied Chemistry Transactions, v. 18, p. 7–14 (in Russian).

Cathelineau, M., Marignac, C., Boiron, M.C., Gianelli, G., and Puxeddu, M., 1994, Evidence for Li-rich brines and early magmatic fluid-rock interactions in the Larderello geothermal system: Geochimica et Cosmochimica Acta, v. 3, p. 1083–1099.

Chester, R., 1990, Marine geochemistry: Londres, Unwyn Hyman, 698 p.

Crawford, M.L., Filer, J., and Wood, C., 1979, Saline fluid inclusions associated with retrograde metamorphism: Bulletin de Minéralogie, v. 102, p. 562–568.

Davies, D.W., Lowenstein, T.K., and Spencer, R.J., 1990, Melting behavior of fluid inclusions in laboratory-grown halite crystals in the systems NaCl-H_2O,NaCl-KCl-H_2O, NaCl-$MgCl_2$-H_2O and NaCl-$CaCl_2$-H_2O: Geochimica et Cosmochimica Acta, v. 54, p. 591–601.

Dubois, M., Royer, J.J., Weisbrod, A., and Shtuka, A., 1993, Reconstruction of low-temperature phase diagrams using a constrained least squares method: Application to the H_2O-CsCl system: European Journal of Mineralogy, v. 5, p. 1145–1152.

Dupuis, T., 1958, Magnésium, *in* Pascal, P., ed., Nouveau traité de chimie minérale: Paris, Masson, v. 4, p. 135–279.

Fouquet, Y., Stackelberg, U.V., Charlou, J.L., Donval, J.P., Erzinger, J., Foucher, J.P., Herzig, P., Mühe, R., Soakai, S., Wiedlicke, M., and Whitechurch, H., 1991, Hydrothermal activity and metallogenesis in the Lau back-arc basin: Nature, v. 349, p. 778–781.

Fouquet, Y., Stackelberg, U.V., Charlou, J.L., Erzinger, J., Herzig, P.M., Mühe, R., and Wiedicke, M., 1993, Metallogenesis in back-arc environments: The Lau basin example: ECONOMIC GEOLOGY, v. 88, p. 2154–2181.

Fouquet, Y., Dubois, M., Marignac, C., and Ramboz, C., 1994, Apport des inclusions fluides à la connaissance de l'hydrothermalisme du Bassin de Lau (Océan Pacifique) [abs.]: Réunion des Sciences de la Terre Conference, 15th, Nancy, (France), April 26–28, Abstracts, p. 105.

Fujino, K., Lewis, E.L., and Perkins, R.G., 1974, The freezing point depression of sea water at pressures up to 100 bars: Journal of Geophysical Research, v. 79, p. 1792–1797.

Gibbard, H.F., and Gossmann, A., 1974, Freezing points of electrolyte solutions. I. Mixtures of sodium chloride and magnesium chloride in water: Journal of Solution Chemistry, v. 3, p. 385–394.

Hall, D.L., Sterner, S.M., and Bodnar, R.J., 1988, Freezing point depression of H_2O-KCl-NaCl solutions: ECONOMIC GEOLOGY, v. 83, p. 197–202.

Hanor, J.S., 1994, Origin of saline fluids in sedimentary basins: Geological Society Special Publication, v. 78, p. 151–174.

Haynes, F.M., 1985, Determination of fluid inclusion composition by sequential freezing: ECONOMIC GEOLOGY, v. 80, p. 1436–1439.

Johnson, R.A., and Wichem, D.W., 1982, Applied multivariate statistical analysis: Englewood Cliffs, New Jersey, Prentice-Hall Inc., 594 p.

Keitel, H., 1923, Systems KCl-$MgCl_2$-H_2O and NaCl-$MgCl_2$-H_2O: Kali-Forschungsanstalt, v. 17. p. 1954–1965.

Khitrova, V.A., 1954, Polytherms of the ternary $NaNO_3$-NaCl-H_2O: Zhurnal Prikladnoj Khimii, v. 27. p. 1281–1289 (in Russian).

Kournakov, N.S., and Zemcuznyj, S.E., 1924, Equilibrium of the reciprocal system NaCl-$MgSO_4$ in application to natural brines: Anorganische und Allgemeine Chemie Zeitschrift, v. 140, p. 149–182.

Linke, W.F., 1958, Solubilities of inorganic and metal-organic compounds. New York, Van Nostrand. 1407 p.

Luzhnaja, N.S., and Vereshtchetina, I.P., 1946, Solubility polytherms of sodium chloride, calcium chloride and magnesium chloride in aqueous solutions from −57° to +25°C: Zhurnal Prikladnoj Khimii, v. 19, p. 723–733 (in Russian).

Marignac, C., Lécuyer, C., Dubois, M., Fouquet, Y., and Ramboz, C., 1995,

Fluid mixing and unmixing in deep-sea hydrothermal systems: The barite-sulphide chimneys of the Lau basin [abs.]: Terra Abstracts, v. 7, p. 211–212.

Mun, A.H., and Darer, P.C., 1957, Cryoscopy of aqueous salt solutions. II. System NaCl-$MgCl_2$-H_2O and KCl-$MgCl_2$-H_2O: Zhurnal Nieorganicesloj Khimii, v. 2, p. 834–837 (in Russian).

Nelson, K.H., and Thompson, T.G., 1954, Deposition of salt from seawater by frigid concentration: Journal of Marine Research, v. 13, p. 3040–3047.

Oakes, C.S., Bodnar, R.W., and Simonson, J.M., 1990, The system NaCl-$CaCl_2$-H_2O: I. The ice liquidus at 1 atm total pressure: Geochimica et Cosmochimica Acta, v. 54, p. 603–610.

Potter, R.W., II, Clynne, M.A., and Brown, D.L., 1978, Freezing point depression of aqueous sodium chloride solutions: ECONOMIC GEOLOGY, v. 73, p. 284–285.

Prutton, C.F., and Tower, O.F., 1932, The system calcium chloride-magnesium chloride-water at 0, −15 and −30°C: American Chemical Society Journal, v. 54, p. 3040–3047.

Ramboz, C., 1980, Géochimie et étude des phases fluides de gisements et indices d'étain-tungstène du sud du Massif Central (France): Unpublished Ph.D. dissertation, Nancy, France, Institut National Polytechnique de Lorraine, 278 p.

Rodebush, W.H., 1918, The freezing points of concentrated solutions and the free energy of solution of salts: American Chemical Society Journal, v. 40, p. 1204–1213.

Roedder, E., 1979, Fluid inclusions as samples of ore fluids, *in* Barnes, H.L., ed., Geochemistry of hydrothermal ore deposits: New York, Wiley Interscience, p. 684–737.

Rüdorff, F., 1861, Über das Gefrieren des Wassers aus Salzlösungen: Annalen für Physikalische Chemie von Poggendorff, v. 114, p. 63–81.

Spencer, T.K., and Lowenstein, R.J., 1992, Phase equilibria in the system H_2O-$MgCl_2$: Pan American Current Research on Fluid Inclusions, 4th, Lake Arrowhead, California, May 22–24, Proceedings, p. 138–141.

Spencer, T.K., Møller, N., and Weare, J.H., 1990, The prediction of mineral solubilities in natural waters: A chemical equilibrium model at temperatures below 25°C: Geochimica et Cosmochimica Acta, v. 54, p. 575–590.

Stephen, H., and Stephen, T., 1963, Solubilities of inorganic and organic compounds: Oxford, Pergamon Press, v. 1, 1933 p.

Sterner, S.M., Hall, D.L., and Bodnar, R.J., 1988, Synthetic fluid inclusions. V. Solubility relations in the system NaCl-KCl-H_2O under vapor-saturated conditions: Geochimica et Cosmochimica Acta, v. 52, p. 989–1005.

Takegami, S., 1921, Reciprocal salt pair NaCl-$MgSO_4$ and Na_2SO_4-$MgCl_2$ at 25°C: Kyoto Imperial University, College of Science, Internal Report, 25 p.

Valori, A., Cathelineau, M., and Marignac, C., 1992, Early fluid migration in a deep part of the Larderello geothermal field: A fluid inclusion study of the granite sill from well Monteverdi: Journal of Volcanology and Geothermal Research, v. 51, p. 115–132.

Vanko, D.A., Bodnar, R.J., and Sterner, S.M., 1988, Synthetic fluid inclusions. VIII. Vapor-saturated halite solubility in part of the system NaCl-$CaCl_2$-H_2O, with applications to fluid inclusions from oceanic hydrothermal systems: Geochimica et Cosmochimica Acta, v. 52, p. 2451–2456.

Williams-Jones, A.E., and Samson, I.A., 1990, Theoretical estimation of halite solubility in the system NaCl-$CaCl_2$-H_2O: Applications to fluid inclusions: Canadian Mineralogist, v. 28, p. 299–304.

Wolff, A.V., Brown, M.G., and Prentiss, P.G., 1986, Concentrative properties of aqueous solutions: Conversion tables, *in* Handbook of chemistry and physics, 67th ed.: Cleveland, CRC Press.

8.3 VEDLEGG 3, ASTM STANDARD D1177 – 94

Designation: D 1177 – 94 (Reapproved 1998)ε1

Standard Test Method for Freezing Point of Aqueous Engine Coolants[1]

This standard is issued under the fixed designation D 1177; the number immediately following the designation indicates the year of original adoption or, in the case of revision, the year of last revision. A number in parentheses indicates the year of last reapproval. A superscript epsilon (ε) indicates an editorial change since the last revision or reapproval.

This standard has been approved for use by agencies of the Department of Defense.

ε[1] NOTE—Footnotes 4 and 5 were updated editorially in May 2003.

1. Scope

1.1 This test method covers the determination of the freezing point of an aqueous engine coolant solution in the laboratory.

NOTE 1—Where solutions of specific concentrations are to be tested, they shall be prepared from representative samples as directed in Test Methods D 1176. Secondary phases separating on dilution need not be separated.

NOTE 2—These products may also be marketed in a ready-to-use form (prediluted).

1.2 The values stated in SI units are to be regarded as the standard. The values given in parentheses are for information only.

1.3 *This standard does not purport to address all of the safety concerns, if any, associated with its use. It is the responsibility of the user of this standard to establish appropriate safety and health practices and determine the applicability of regulatory limitations prior to use.*

2. Referenced Documents

2.1 *ASTM Standards:*

D 1176 Test Method for Sampling and Preparing Aqueous Solutions of Engine Coolants or Antirusts for Testing Purposes[2]

E 1 Specification for ASTM Thermometers[3]

3. Terminology

3.1 *Definitions:*

3.1.1 *freezing point*—the temperature at which crystallization begins in the absence of supercooling, or the maximum temperature reached immediately after initial crystal formation in the case of supercooling.

4. Summary of Test Method

4.1 This test method involves the determination of the time-temperature curve prior to freezing and the determination of the horizontal or flattened portion of the freezing curve. The freezing point is taken as the intersection of projections of the cooling curve and the freezing curve. If the solution supercools, the freezing point is the maximum temperature reached after supercooling.

5. Significance and Use

5.1 The freezing point of an engine coolant indicates the coolant freeze protection.

5.2 The freezing point of an engine coolant may be used to determine the approximate glycol content, provided the glycol type is known.

6. Apparatus

6.1 *Freezing Point Apparatus*, shown assembled in Fig. 1, consisting of the following:

6.1.1 *Cooling Bath*, in which the refrigerant is contained, consisting of a standard 1.9-L (2-qt) Dewar flask.[4] The flask may be silvered or unsilvered, and is supported in a close-fitting container. A pad of glass wool is placed in the bottom of the flask to protect it from damage by tip of freezing tube.

6.1.2 *Freezing Tube*[5] consisting of a 200-mL (6.8-oz.) unevacuated, unsilvered Dewar flask. The tube is closed by a cork having a central hole for the thermocouple or thermometer, a second hole placed to one side for passage of the stirring rod, and a third hole for introducing wire for seeding at appropriate time.

6.1.3 *Stirring Mechanism*, consisting of a five-coil stirrer formed of stainless steel wire 1.6 mm (1⁄16 in.) in diameter. The

[1] This test method is under the jurisdiction of ASTM Committee D-15 on Engine Coolants and is the direct responsibility of Subcommittee D15.03 on Physical Properties.

Current edition approved July 15, 1994. Published September 1994. Originally published as D 1177 – 51T. Last previous edition D 1177 – 93a.

[2] *Annual Book of ASTM Standards*, Vol 15.05.

[3] *Annual Book of ASTM Standards*, Vol 14.03.

[4] A Dewar flask is available on special order from Kimble Glass, Inc., Tel. No. 856–692–3600. Part No. 611430-2124.

[5] For routine work, a tube with a seeding tip as described in the paper by R. E. Mallonee and F. L. Howard, "The Determination of Freezing Point of Engine Antifreeze," in the February 1951 issue of the *ASTM Bulletin* may be used. (See Fig. 2.) A continuous seeding tube, "Mallonee Unevacuated Freezing Point Tube," is manufactured by Custom Glassblowing of Louisville, Inc. Tel. No. 502–239–2215.

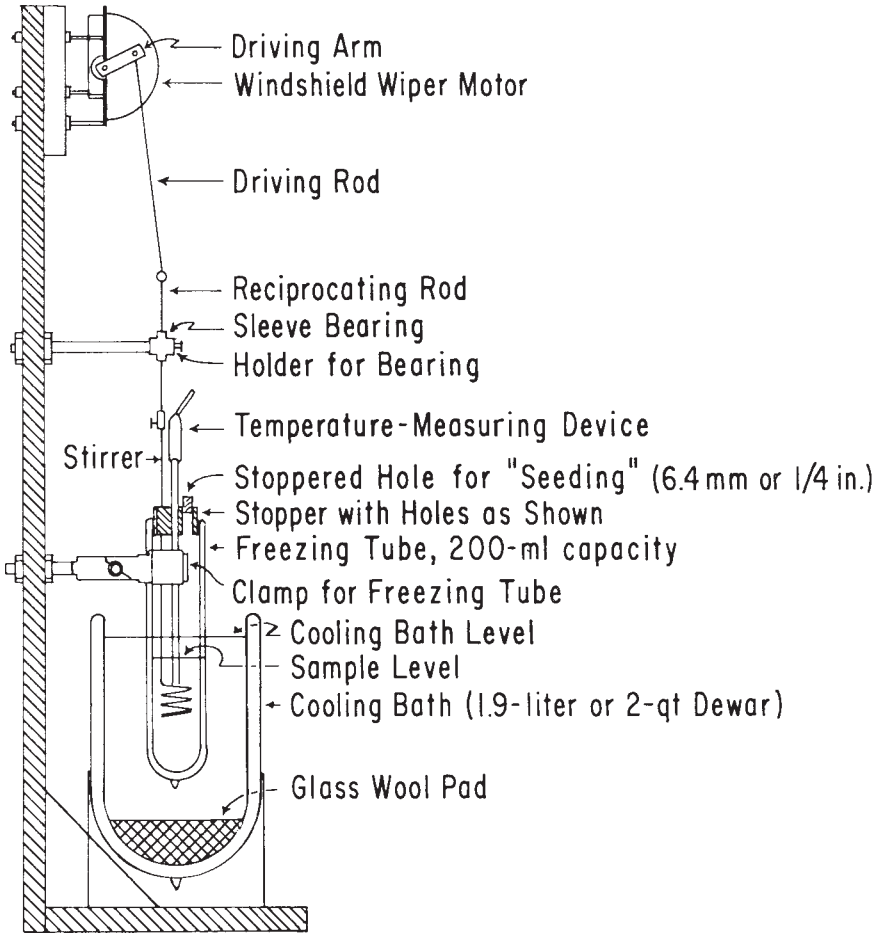

FIG. 1 Assembly of Freezing Point Apparatus

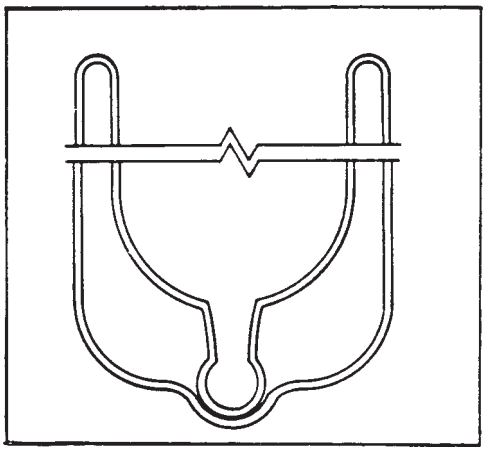

FIG. 2 Bottom of Freezing Tube Showing Seeding Tip

coils are so spaced that, in the extreme upward position during operation, no coils are exposed above the surface of the sample. The stirrer is agitated by means of an ordinary windshield wiper motor or other motor devices, operating through suitable linkages so as to provide linear motion of the stirrer. The length of the stroke is adjusted so that the coil just clears the bottom of the freezing-point tube at low point of the stroke.

6.1.4 *Temperature Measurement*—A resistance thermometer or a multi-junction copper-constantan thermocouple may be used with suitable measuring instruments, providing these give an over-all sensitivity of 0.1°C (0.2°F). The instrument shall be calibrated before each series of determinations by using suitable reference standards. Platinum resistance thermometers have been adopted as a standard by the National Institute of Standards and Technology (NIST) and are recommended for this standard.

NOTE 3—ASTM Coolant Freezing Point Thermometer having a range from − 37 to + 2°C (−35 to + 35°F) or − 54 to − 15°C (−65 to + 5°F) and conforming to the requirements for Thermometers 75C or 76C as prescribed in Specifications E 1, may be used where less accuracy is acceptable provided reference standards are used for calibration purposes.

7. Refrigerant

7.1 The refrigerant shall consist of solid carbon dioxide in alcohol or in other suitable bath liquids.

NOTE 4—A layer of dry ice, at least 13 mm (½ in.) thick, must be maintained in the bottom or on the top of the cooling bath during a determination, depending on the bath liquid used. Adequate precautions should be taken against fire hazards or toxic effects of bath liquids, or both.

7.2 Liquid nitrogen may be used as the refrigerant when the freezing point of the coolant is − 46°C (−50°F) or lower.

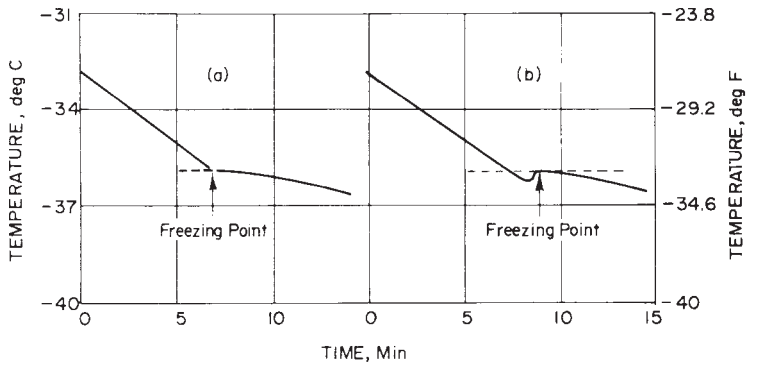

FIG. 3 Time-Temperature Cooling Curves for Determining the Freezing Point of an Engine Coolant

NOTE 5—**Warning:** The liquid nitrogen should be discarded after each day's use to avoid the possibility of explosion due to dissolved oxygen and inadvertent mixing with organic coolant materials.

8. Procedure

8.1 Assemble the apparatus as shown in Fig. 1, with no refrigerant and no sample of coolant yet in place. Check the operation of the stirring mechanism after assembly to be sure that all parts operate freely.

8.2 Fill the Dewar flask surrounding the freezing tube with the refrigerant liquid, adding pieces of solid carbon dioxide from time to time to maintain conditions mentioned in Note 4. Temporarily remove the stopper from the freezing tube and introduce 75 to 100 mL (2.65 to 3.4 oz.) of the sample.

NOTE 6—The sample may be precooled to approximately 8°C (15°F) above the expected freezing point before introducing it into the freezing tube.

8.3 Start the stirrer and adjust it to operate at 60 to 80 strokes per min (Note 7). As soon as stirring is begun, observe and record the temperature at regular intervals of time. As the expected freezing point is approached, the time intervals should be quite short, 15 s if possible. At the expected freezing point, seeding should be started to prevent supercooling. This can be accomplished by introducing a wire which has a small portion of the solution being tested frozen on its tip. It is most convenient to freeze this solution in a small test tube inserted directly into the cooling bath.

NOTE 7—A stroke is considered as a complete cycle of one upward and one downward motion of the stirrer.

NOTE 8—The cooling rate must be less than 1°C (2°F)/min at the time the solution is seeded.

8.4 Continue temperature readings at regular intervals for at least 10 min after the apparent freezing point.

9. Report

9.1 Plot the observed temperature against time on rectangular coordinate paper. Where the curve shows a definite flat or plateau during freezing, the freezing point is taken as the intersection of projections of the cooling curve and the flat or horizontal plateau portion of the freezing curve (see Fig. 3(*a*)). If the solution supercools, the freezing point is the maximum temperature reached immediately after supercooling (see Fig. 3(*b*)).

NOTE 9—The amount of supercooling should be held to a minimum. If the supercooling exceeds 1°C (2°F) the test should be rejected.

10. Precision and Bias

10.1 *Precision*—The precision of this test method, as determined by the examination of the interlaboratory test results, is as follows:

10.1.1 *Repeatability*— Results obtained by one operator and one apparatus should not differ from the mean by more than ±0.3°C (±0.5°F).

10.1.2 *Reproducibility*— Results obtained by different operators and different apparatuses should not differ from the mean by more than ±0.6°C (±1.0°F).

10.2 *Bias*—Since there is no acceptable reference material suitable for determining the bias for the procedure in this test method bias has not been determined.

11. Keywords

11.1 aqueous engine coolants; engine coolants; engine coolants; freezing point

SINTEF Energiforskning AS
Adresse: 7465 Trondheim
Telefon: 73 59 72 00

SINTEF Energy Research
Address: NO 7465 Trondheim
Phone: + 47 73 59 72 00